horticulturae

MDPI

Article

Satureja montana Essential Oil, Zein Nanoparticles and Their Combination as a Biocontrol Strategy to Reduce Bacterial Spot Disease on Tomato Plants

Paulo R. Oliveira-Pinto [1,2,*], Nuno Mariz-Ponte [1,2,3], Rose Marie O. F. Sousa [1,4,5], Ana Torres [1], Fernando Tavares [1,3], Artur Ribeiro [6], Artur Cavaco-Paulo [6], Manuel Fernandes-Ferreira [1,4,5] and Conceição Santos [1,2]

1 Department of Biology, Faculty of Sciences, University of Porto, 4169-007 Porto, Portugal; nuno.ponte@fc.up.pt (N.M.-P.); rose.sousa@fc.up.pt (R.M.O.F.S.); up201505894@fc.up.pt (A.T.); ftavares@fc.up.pt (F.T.); manuel.ferreira@fc.up.pt (M.F.-F.); csantos@fc.up.pt (C.S.)
2 LAQV-REQUIMTE, Faculty of Sciences, University of Porto, 4169-007 Porto, Portugal
3 CIBIO-InBIO, Campus de Vairão, Universidade do Porto, Rua Padre Armando Quintas, 4485-661 Vairão, Portugal
4 GreenUPorto, Faculty of Sciences, University of Porto, Rua Campo Alegre, 4169-007 Porto, Portugal
5 CITAB, Centre for the Research and Technology of Agro-Environmental and Biological Sciences, Universidade de Trás-os-Montes e Alto Douro, 5000-801 Vila Real, Portugal
6 Centre of Biological Engineering, Campus de Gualtar, University of Minho, 4710-057 Braga, Portugal; arturibeiro@ceb.uminho.pt (A.R.); artur@deb.uminho.pt (A.C.-P.)
* Correspondence: up201606827@edu.fc.up.pt

check for updates

Citation: Oliveira-Pinto, P.R.; Mariz-Ponte, N.; Sousa, R.M.O.F.; Torres, A.; Tavares, F.; Ribeiro, A.; Cavaco-Paulo, A.; Fernandes-Ferreira, M.; Santos, C. *Satureja montana* Essential Oil, Zein Nanoparticles and Their Combination as a Biocontrol Strategy to Reduce Bacterial Spot Disease on Tomato Plants. *Horticulturae* **2021**, *7*, 584. https://doi.org/10.3390/horticulturae7120584

Academic Editor: TaeJin Cho

Received: 16 November 2021
Accepted: 14 December 2021
Published: 16 December 2021

Abstract: Tomato bacterial spot (Bs), caused by *Xanthomonas* spp., including *X. euvesicatoria* (Xeu) remains a major threat for tomato production. The emergence of copper resistance strains of Xeu calls urgently for eco-friendly phytosanitary treatments as sustainable green alternatives for disease control. *Satureja* spp. essential oil (EO) has antimicrobial activity against xanthomonads and combined with zein nanoparticles (ZNPs), might offer a viable option for field applications. This study aims to evaluate the effects of *S. montana* EO, of ZNPs, and their combination in a nanoformulation, on Xeu quantity, and how these compounds modulate molecular and physiological changes in the pathosystem. Uninfected and infected tomato plants (var. Oxheart) were treated with EO; ZNPs and nanoformulation (EO + ZNPs). Treatments reduced Xeu amount by a minimum of 1.6-fold (EO) and a maximum of 202-fold (ZNPs) and improved plants' health. Nanoformulation and ZNPs increased plants' phenolic content. ZNPs significantly increased GPX activity and reduced CAT activity. Overall treatments upregulated transcripts of the phenylpropanoid pathway in infected plants, while ZNPs and nanoformulation upregulated those transcripts in uninfected plants. Both *sod* and *aao* transcripts were downregulated by treatments in infected plants. These findings demonstrate that *S. montana* EO, ZNPs and their nanoformulation are suitable to integrate tomato bacterial spot management strategies, mainly due to their antimicrobial activity on Xeu, however further field studies clarifying the long-term action of these products are required. These results also support the prophylactic potential of ZNPs on tomato bacterial spot.

Keywords: *Satureja montana*; essential oil; zein nanoparticles; nanoformulation; bacterial spot; *Solanum lycopersicum*; *Xanthomonas euvesicatoria*

1. Introduction

Tomato (*Solanum lycopersicum* L.) is one of the world's most consumed and produced fresh vegetables [1], with 180 million tonnes being produced globally in 2019, according to FAOSTAT (www.fao.org, accessed on 10 August 2021). Currently, tomato production is affected by several bacterial diseases, among which is the bacterial spot (Bs). This disease can lead to significant yield losses [2]. Bs can be caused by four species of the *Xanthomonas*

genus (*X. vesicatoria*; *X. euvesicatoria*; *X. gardneri*; *X. perforans*) [3]. Among these four species, only *X. euvesicatoria* (Xeu) and *X. vesicatoria* can cause disease symptoms on fruits [3]. Plants infected with Bs show small, irregular dark lesions that eventually make the leaves turn yellow and may lead to plant defoliation. Several plant organs can be affected by Bs, including stems, leaves, and fruits [4,5].

Current disease management strategies are focused on the application of copper-based bactericides and in some countries also of antibiotics [6,7]. However, the emergence of copper resistant Xeu strains has been widely reported [8]. A combination of mancozeb and Cu-based bactericides has been recommended, but the application of this combined treatments did not improve disease management [9]. Furthermore, the European Union has issued directives forbidding the use of antibiotics to control phytopathogens, and it also leans towards replacing copper with green alternatives that can be integrated in organic farming systems without limitations, mainly due to copper's phytotoxicity and non-target effects (i.e., soil accumulation) [10].

Thus, in recent years, emergent sustainable and eco-friendly products/formulations to manage plant diseases have been evaluated [11–13]. For example, the application of plant extracts/essential oils (EOs), silicates and microbial metabolites that are capable of inducing plant's resistance when applied to the leaves have been reported [14,15]. EOs have been highlighted for their potential to control a myriad of plant pathogens [16,17], namely xanthomonads-causing bacterial spots [18,19]. EOs are complex mixtures of volatile compounds obtained from several organs/structures of aromatic and medicinal plants [20]. These natural products have well characterized antimicrobial activities [21], with carvacrol and linalool being the key molecules that confer such activities [22–24]. Despite these antimicrobial properties, most studies on phytopathogens have been performed in vitro conditions [25,26] thus evidence for the potential of these products for disease management under field conditions are sparse.

Satureja montana, commonly known as winter savory, is a medicinal plant that belongs to the Laminaceae family, an economically relevant plant taxon mainly due to its essential oil (EO) production capacity [27]. *S. montana* is a perennial plant that grows in many European countries, particularly in warm rocky areas of the Mediterranean and in some countries of the Middle East [28,29] www.cabi.org/ (accessed on 1 August 2021). *S. montana* EO is known for its antimicrobial and antifungal activities [30,31]. Terpenoids (carvacrol and linalool) are abundant in this species' EO, accounting for the antimicrobial capabilities mentioned above [29]. Note that EOs obtained from the *Satureja* genus have already been shown to have bactericidal effect against xanthomonads, namely *X. axanopodis* pv. *malvacearum*, pv. *vesicatoria*, pv. *vitians*, pv. *pelargonii* and pv. *campestris*, *X. campestris* pv. *raphanin* and pv. *zinniae* [32]. However, *S. montana* has not been tested against Xeu, including *in planta* conditions (*S. lycopersicum*) and therefore, its efficiency for Bs management remains unknown.

EO application in field conditions present many obstacles due to the volatility of most compounds [33]. Recent studies demonstrated that nanoparticle (NP)-encapsulated EOs have increased antimicrobial potential against multi-resistant pathogens due to an increase in EOs' chemical stability and solubility [23]. Zein nanoparticles are a suitable candidate for the establishment of a NP-EO nanoformulation due to their coating capacity, biodegradability, and biocompatibility [34]. Zein is the major protein present in maize (*Zea mays*) and it is composed of lipophilic aminoacidic residues, consequently it can be easily converted into spherical, colloidal nanoparticles [35,36]. These zein-NPs were already used as nanodelivery systems for carvacrol, one of the major compounds in *S. montana* EOs and improved its bioactivity [37,38]. EO-Zein nanoformulations have also been tested, with results indicating an enhancement of EO's stability and antimicrobial activity against pathogenic bacteria [39]. Zein-NPs have demonstrated a non-toxic profile when applied to plants, for example, the application in beans did not compromise the plants' growth [40].

The current challenges on tomato phytopathogen management have created a need for green solutions that could be effectively applied in field conditions against tomato

pathogens. *S. montana* EO is a promising candidate to integrate natural products that can successfully reduce Xeu damages on tomato plantations, since *Satureja* sp. has shown successful applications to control Bs on tomato [32]. This, together with the effectiveness of zein NPs as EO nanocarriers and as activity enhancers [39] raises the hypothesis to combine these products and explore their activity against Xeu in *S. lycopersicum*.

This study aims to quantify the efficacy of *S. montana* EO, free or encapsulated in Zein NPs on Xeu population and assess EOs effects on Xeu-tomato pathosystem at a molecular and physiological level. This work provides new insight about the effectiveness of *S. montana* EO and zein coating in planta conditions to control Xeu, and the action mechanisms related to plants' response, ultimately leading to the application of this strategy to control Bs in tomato.

2. Materials and Methods

2.1. Essential Oil Obtention, Synthesis of Zein Nanoparticles, and EO-Zein NPs

Essential oil from *Satureja montana* obtained from steam distillation was purchased from Florihana distillerie (Caussols, France). An analytical balance (VWR, Radnor, PA, USA) was used to assess EO density ($\rho EO = 1.02$ g cm^{-3}). *S. montana* EO is mainly composed of carvacrol (43%), *p*-cymene (17%), γ-terpinene (13%) and thymol (4%) (data not shown). Zein NPs were prepared using an anti-solvent precipitation method [41]. Shortly, 500 mg of zein (Sigma, Madrid, Spain) were dissolved in 70% ethanol with constant stirring until the solution became clear. For the preparation of EO-Zein nanoparticles, 500 mg of *S. montana* EO were added to the solution and stirred for 5 min at 250 rpm. The EO-Zein solution was rapidly dispersed at high speed into deionized water until a single phase was formed. The solution containing the encapsulated EO particles was kept at 4 °C after separation of the non-encapsulated *S. montana* EO using a PD-10, Sephadex™ G-25 column (Cytiva, Marlborough, MA, USA). Zein particles without EO were also prepared as described previously.

The stability of the NPs during storage (12 weeks at 4 °C) was followed by the evaluation of particle size, surface charge and polydispersion index (PDI) using the DLS-dynamic light scattering method (Zetasizer, Nano-ZS, Malvern Instruments, Malvern, UK).

The efficiency of NP formation was assessed by separation of the free protein from the NPs, using 100 kDa centrifugation Amicon tubes. The free protein was quantified by detergent compatible (DC™) colorimetric method (DC™ colorimetric kit, BioRad, Amadora, Portugal). A calibration curve was performed with BSA (ranging from 0.05 mg mL^{-1} to 2 mg mL^{-1}). Absorbance was recorded at 750 nm. The efficiency of particle formation was determined by the following equation:

$$Eff.\ particles\ (\%) = \frac{[Protein]i - [Protein]f}{[Protein]f} \times 100$$

where *Eff. particles (%)* is the efficiency of particle formation; [*Protein*]*i*, the protein concentration used to prepare the NPs and [*Protein*]*f* stands for the free protein concentration quantified by the DC™ Protein Assay.

The efficiency of EO encapsulation was assessed by spectrophotometric quantification of the non-encapsulated EO. Free EO separation from NP solution was conducted using a PD-10, Sephadex™ G-25 column, followed by a solvent extraction step with ethyl-acetate. Extracts' absorbance was recorded at 275 nm. A calibration curve of *S. montana* EO in ethyl-acetate was performed ($R^2 = 0.9885$).

2.2. Plant Growth Conditions and Treatments

Seeds of *S. lycopersicum* var. Oxheart were obtained from a commercial supplier (Vilmorin, France). Germination was performed in 80 cm^3 seed starter trays with a commercial substrate (Siro, Mira, Portugal). Plants were kept in a plant-growth chamber at 24 ± 2 °C and 50 ± 10% (relative humidity) RH, with a photosynthetic light intensity of 250 µmol m^{-2}s^{-1} and 16:8 h (light:dark) photoperiod. 10 days after germination, the seedlings were transferred

to 0.9 dm^3 pots (one plant per pot) with the same substrate. 45-day-old plants were divided in groups corresponding to each treatment as follows (Figure 1), (1) CBC-uninfected/untreated; (2) CBX-Xeu-infected/untreated; (3) CBS-uninfected/*S. montana* EO (0.4 mg mL^{-1} in 8% (*w*/*v*) ethanol); (4) CBSZ-uninfected/*S. montana* EO-zein NPs (0.4 mg mL^{-1} EO, incorporated in 1.6 mg mL^{-1} zein); (5) CBZ-uninfected/zein NPs (1.6 mg mL^{-1}); (6) CBXS-Xeu-infected/*S. montana* EO (0.4 mg mL^{-1} in 8% (*w*/*v*) ethanol); (7) CBXSZ-Xeu-infected/*S. montana* EO-zein NPs (0.4 mg mL^{-1} EO, incorporated in 1.6 mg mL^{-1} zein); (8) CBZ-Xeu-infected/zein NPs (1.6 mg mL^{-1}). CBC and CBX were used as controls throughout the experiments.

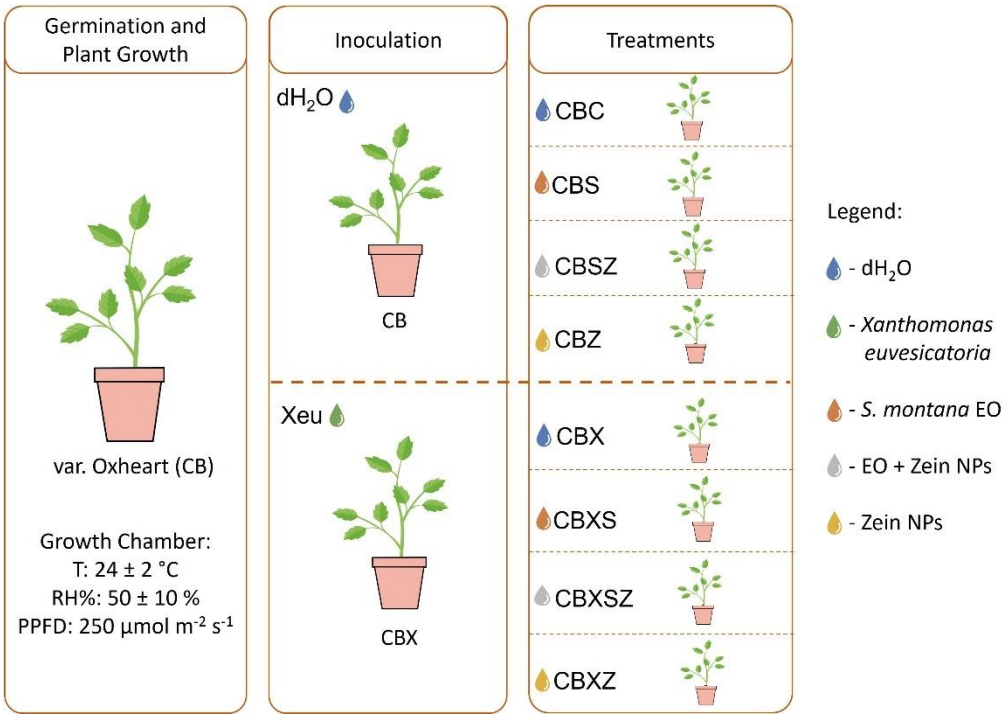

Figure 1. Schematic representation of the treatments applied to tomato plants.

X. euvesicatoria LMG 905 were grown at 28 °C in yeast extract-dextrose-$CaCO_3$ (YDC) medium. Infection was carried out in 45-day-old plants by inoculation with 4 mL of a suspension of *X. euvesicatoria* (LMG 905) at and optical density (λ = 600 nm) of 0.25. The bacterial suspension was applied by spraying both leaf sides with a spray vial. After inoculation, the plants were enclosed for 24 h in transparent polythene bags to create a high relative-humidity atmosphere and facilitate pathogen penetration. Treatments were applied 2 days after infection following the groups established above, by spraying both leaf sides with approximately 3 mL of treatment solution per plant, sterile deionized water was used for the controls (CBC and CBX). Ten days after treatments, three leaves from the third node of each plant were removed, ground in liquid nitrogen and preserved at −80 °C for further analysis. In this experiment, three biological plants/replicates were done for each treatment.

2.3. Xeu Quantification

To quantify *Xeu* population present in tomato leaves, total RNA was extracted from 100 mg of leaf samples using NZYol (NZYTech™, Lisboa, Portugal) according to the manufacturers' protocol. Samples were treated with DNaseI (NZYTech™) according to the manufacturers' instructions. cDNA synthesis and RNase treatment were performed following NZY First-Strand cDNA Synthesis Kit (NZYTech™) in conformity with the manufacturers' established protocol. A conventional PCR reaction was performed to detect the presence of Xeu, using primers for bacterial quantification through RT-qPCR [42]: xeu2.4-

CTGGGAAACTCATTCGCAGT (forward) and xeu2.5–TTGTGGCGCTCTTAT TTCCT (reverse), with a product size of 208 bp. Amplification conditions were as follows, an initial denaturation of 1 min at 95 °C, followed by 45 cycles of 15 s of denaturation at 95 °C, 15 s of annealing at 60 °C and 15 s of extension at 72 °C, and finalized by a 7 min final extension at 72 °C. Samples were then loaded in a 1% (*w*/*v*) agarose gel, in TBE buffer and ran for 30 min at 90 V.

Xeu was quantified by RT-qPCR, using the CFX96™ Real-Time PCR Detection System (BioRad, Hercules, CA, USA). Each reaction used 10 µL of NZYSpeedy qPCR Green Master Mix (2×), ROX plus (NZYTech™), 0.8 µL of forward primer (10 mM), 0.8 µL of reverse primer (10 mM), 0.4 µL of DEPC treated water and 8 µL of cDNA template. Amplification conditions were as follows, 1 min of denaturation at 95 °C, 45 cycles of 5 s at 95 °C and 15 s at 60 °C. Melting curve analysis ranged from 65 °C to 95 °C with temperature increasing 0.5 °C in each cycle (5 s per cycle). A standard curve was performed using Xeu LGM 905 template, serial dilutions were performed from an initial stock of 10^8 cells down to 10^1 cells. qPCR reactions were performed in triplicates and concurrently with the standard curve. Primer efficiency was calculated using the Real-time PCR miner, and the efficiency values were used to obtain the Cq values of each amplification curve [43]. The standard curve (R^2 = 0.994) was used to quantify Xeu in leaf samples.

2.4. Quantification of Reactive Oxygen Species

2.4.1. H_2O_2 Concentration in Leaves

Hydrogen peroxide was quantified spectrophotometrically [44]. Leaf tissue (50 mg) was macerated in 1 mL of TCA 0.1% (*w*/*v*) using a Bead Ruptor 12 Homogenizer (OMNI International, Kennesaw, GA, USA). Another 1 mL of TCA 0.1% (*w*/*v*) was added to the homogenate and samples were briefly vortexed (5 s at maximum speed) using a VWR Analog Vortex Mixer (Radnor, PA, USA). After centrifugation (12,000× *g*, 15 min, 4 °C), 500 µL of supernatant were mixed with 500 µL phosphate buffer 0.1 M (pH = 7) and 1 mL of potassium iodide (KI) 1 M. The mixture was homogenized using an Analog Vortex Mixer (VWR, Radnor, PA, USA) for 5 s at maximum speed and incubated in the dark, at room temperature for 60 min. Absorbances were recorded at 390 nm using a Multiskan™ GO Microplate Spectrophotometer (Thermo Scientific™, Waltham, MA, USA). A standard curve was made with known concentrations of hydrogen peroxide (from 0 up to 100 µM) R^2 = 0.999, and results were expressed as mmol of H_2O_2 per g of fresh weight (FW).

2.4.2. Superoxide Radical Concentration in Leaves

The superoxide radical was semi-quantified following Gajewska et al. [45], with the modifications described by Costa-Santos et al. [46]. Briefly, 50 mg of leaf tissue was homogenized in 2 mL of extraction buffer, consisting of phosphate buffer 0.01 M (pH = 7.8), 0.05% (*w*/*v*) of nitroblue tetrazolium (NBT) dissolved in 100 µL of DMSO (dimethyl sulfoxide) and 10 mM sodium azide. Samples were incubated in the dark, at room temperature for 1 h, with occasional inversions. Samples were centrifuged (VWR, Radnor, PA, USA) at 13,000× *g* for 2 min at 4 °C. Supernatant (1.5 mL) was collected and incubated at 85 °C for 10 min. Samples were then chilled on ice to stop the reaction. Absorbance was recorded at 580 nm using the Thermo Scientific™ Multiskan™ GO Microplate Spectrophotometer and results were presented as absorbance (Abs) per g of FW.

2.5. Non-Enzymatic Antioxidant Capacity (NEAC)

2.5.1. Total Phenol Content Quantification

To quantify the total phenols, present in leaf samples, the protocol established by Dewanto et al. [47] was followed. Thus, 50 mg of powdered leaf tissue were homogenized in 3 mL of an aqueous solution of 10% methanol (*v*/*v*), using a Bead Ruptor 12 Homogenizer (OMNI International). Homogenates were vacuum-filtered through qualitative paper on a Büchner funnel. After centrifugation (2500 rpm, 10 min, 4 °C) 125 µL of the supernatant were added to 500 µL of extraction buffer and 125 µL of the Folin-Ciocalteu reagent, the

mixture was homogenized by vortexing (VWR, Radnor, PA, USA) for 5 s at maximum speed and incubated for 6 min at room temperature. Then, 1250 µL of Na_2CO_3 7% (*w*/*v*) and 1 mL of deionized H_2O were added to the mixture and homogenized by vortexing with the Analog Vortex Mixer (VWR, Radnor, PA, USA) for 10 s at maximum speed. Samples were incubated in the dark, at room temperature for 90 min and absorbance was recorded at 760 nm using the using the Thermo Scientific™ Multiskan™ GO Microplate Spectrophotometer. A standard curve was made with known concentrations of gallic acid (Sigma-Aldrich, St. Louis, MO, USA) (from 0 up to 500 µg mL^{-1}) and results were presented as µg of gallic acid equivalents (GAE) per g of FW.

2.5.2. Antiradical Activity

The method described by Harkat-Madouri et al. [48] was used to determine the antiradical activity of leaf extracts based on the (2,2-diphenyl-1-picrylhydrazyl) DPPH-scavenging activity. Briefly, 50 mg of leaf tissue were macerated in 3 mL of 90% (*v*/*v*) methanol using a Bead Ruptor 12 Homogenizer (OMNI International) and the homogenates were filtered through qualitative paper on a Büchner funnel under vacuum. Extracts were then centrifuged at 2500 rpm for 10 min at 4 °C, then 100 µL of supernatant were mixed with 100 µL of extraction buffer and 1250 µL of DPPH 0.2 mM. The mixture was homogenized and incubated in the dark, at room temperature for 30 min. Absorbance was recorded at 517 nm using the Thermo Scientific™ Multiskan™ GO Microplate Spectrophotometer. For the standard curve, known concentrations of gallic acid ranging from 0 to 0.5 mg mL^{-1} (R^2 = 0.9846). Results were presented as µg of gallic acid equivalents (GAE) per mL of extract.

2.6. Antioxidant Enzyme Activity

The activity of key-antioxidant enzymes was assessed following the protocols of Mariz-Ponte et al. [49] for tomato leaves. Therefore, 100 mg of leaf tissue was macerated with 1.5 mL of extraction buffer, consisting of phosphate buffer 0.1 M (pH = 7.4), EDTA (ethylenediamine tetraacetic acid) 1 mM, 0.2% (*w*/*v*) TritonX, DTT (dithiothreitol) 2 mM, PMSF (phenylmethylsulfonyl fluoride) 1 mM and 2% (*w*/*v*) PVP (polyvinylpyrrolidone), in a bead mill homogenizer (MM400, Retsch, Haan, Germany) at a shaking frequency of 30 s^{-1} in cold conditions. After homogenization, samples were centrifuged for 15 min at 8000× *g*, 4 °C.

The total soluble protein content of the samples (TSP) was determined following the Bradford method [50], by adding 5 µL of supernatant to 150 µL of Bradford reagent (Sigma-Aldrich). Samples were incubated for 10 min at room temperature and the absorbance was recorded at 595 nm using a Thermo Scientific™ Multiskan™ GO Microplate Spectrophotometer. A standard curve was made with known concentrations of bovine serum albumin (BSA) (0 to 1.2 mg mL^{-1}) with an R^2 of 0.998. Results were expressed as mg of protein per g of fresh weight. Concerning the quantification of the activity of guaiacol peroxidase (GPX), 100 µL of supernatant were mixed with 100 µL of phosphate buffer 0.1 M (pH = 7), 15 µL of guaiacol 15 mM and 50 µL of H_2O_2 3 mM. After a 10 min incubation in the dark, at room temperature, absorbance was recorded at 470 nm using a Thermo Scientific™ Multiskan™ GO Microplate Spectrophotometer and results were expressed as mmol $mgProt^{-1}$. To determine the activity of catalase (CAT), 60 µL of supernatant were added to 135 µL of phosphate buffer (pH = 7) and 50 µL of H_2O_2 0.083 M. Absorbance was recorded at 240 nm 12 times, every 10 s, using a Thermo Scientific™ Multiskan™ GO Microplate Spectrophotometer. Results were expressed as nanokatal (nKat) per µg of protein. Finally, to quantify superoxide dismutase (SOD), 940 µL of reaction buffer (phosphate buffer 0.1 M (pH = 7.8), methionine 70 mM, EDTA 10 µM, NBT 1 mM and ultra-pure water, were mixed with 50 µL of supernatant and 50 µL of riboflavin (2 mM). Samples were divided in 2 sets, one was incubated, in the dark, and another under a light bulb for 10 min. Absorbance was recorded at 560 nm using a Thermo Scientific™

Multiskan™ GO Microplate Spectrophotometer and results were expressed in SOD units (U) per mg of fresh weight.

2.7. Gene Expression Analysis

To evaluate leaves' gene expression levels, 100 mg of powdered leaf tissue was homogenized in NZYol (NZYTech™) for total RNA extraction, following the manufacturer's instructions. After RNA isolation, samples were digested with NZY DNase I (NZYTech™) and cDNA was synthesized using the NZY First-Strand cDNA Synthesis Kit (NZYTech™) according to the manufacturer's guidelines. cDNA was diluted (1:10) in MilliQ water and stored at −20 °C. Two housekeeping genes, ubiquitin (*ubi*) and tubulin (*tub*) (Table 1) were used to normalize the relative expression levels and transcripts related to biotic stress defense pathways were quantified by RT-qPCR: (1) hormone response: oxophytodienoate reductase 3 (*opr3*), and ABA aldehyde oxidase (*aao*); (2) flavonoid/anthocyanin pathways: phenylalanine ammonia-lyase 5 (*pal5*), chalcone synthase 1 (*chs1*), dihydroflavonol reductase (*dfr*) and flavonol synthase (*fls*); (3) carotenoid synthesis: carotenoid isomerase (*crtiso*); (4) antioxidant activity: cytosolic ascorbate peroxidase (*apxcyto*) and superoxide dismutase (*sod*).

Table 1. Primers used for gene expression analysis.

Gene.	Primer	Sequence	Annealing Temperature (°C)	Product Size (bp)	Reference
ubi	Forward Reverse	GGACGGACGTACTCTAGCTGAT AGCTTTCGACCTCAAGGGTA	60	134	[51]
tub	Forward Reverse	AACCTCCATTCAGGAGATGTTT TCTGCTGTAGCATCCTGGTATT	60	180	[51]
crtiso	Forward Reverse	GTTTGTAATCTTGGGTTTCCAGCA TTGCCTTGTGGGTTTCAAGC	60	117	This Study
fls	Forward Reverse	ATAGCTCCACAACCAGGTGC TCCATTTGGCCTCACCACTC	60	108	[52]
dfr	Forward Reverse	TGCCCTTTCACTAATTACCGCT CCTTGGGGTGCTCATACAGG	60	107	This Study
pal5	Forward Reverse	TGGAGGAGAATTTGAAGAATGCTG TCCCTTTCCACCACTTGTAGC	60	136	This Study
chs1	Forward Reverse	ACCAACAAGGTTGCTTTGCC GAGATTCACTGGGTCCACGG	60	135	[52]
apxcyto	Forward Reverse	GTTGAAGGTCGCTTGCCG CCAAGGTATGGGCACCAG	60	118	[53]
sod	Forward Reverse	GCCACTGCCTCTGCTAATTCA CCAAATTGTTTCTTTTGGGTTCTCC	60	104	[52]
aao	Forward Reverse	CCAGGCACAAACACAATCAA GTCGTAAATAATATCAGACTG	60	154	[54]
opr3	Forward Reverse	ATGGACTCTAATCCACTCAGCCTTG TCACTGCCAAGTCTGCCTGCTTCAG	60	152	[55]

Real-time quantitative polymerase chain reactions (RT-qPCR) were performed using a CFX96 Touch™ thermocycler (Bio-Rad). For each reaction, 2.5 µL of total first-strand cDNA, 10 µL of NZYSpeedy qPCR Green Master Mix (2×), ROX plus (NZYTech™), 0.8 µL of each primer (forward and reverse) and 5.9 µL of MilliQ water were used. Amplifications were standardized as follows: 95 °C for 1 min followed by 50 cycles of 5 s at 95 °C and 15 s at 60 °C. The melting curve analysis ranged from 65 °C to 95 °C with an increment of 0.5 °C per each 5 s/cycle. Real-time PCR miner [43] was used to calculate the efficiency of the primers and determine the Cq values.

2.8. Statistical Analysis

Three biological replicates were used per condition and treated as pools. Comparisons between treatments were made using One-way ANOVA test (GraphPad™ Prism 9,

company, San Diego, CA, USA). The Dunnett Comparison Test ($p < 0.05$) was also applied to assess the statistical significance of the data. The MixOmics package for R software (R Foundation for Statistical Computing, Vienna, Austria) was used for the PCA biplot with confidence ellipses (0.95).

3. Results

3.1. NP Formation Efficiency, EO Encapsulation Efficiency and NP Stability during Storage

After synthesis of Zein nanoparticles, and encapsulation of *S. montana* EO, the NP formation efficiency and the EO encapsulation efficiency were determined. NP formation efficiencies were 80.08 ± 2.32% for the EO-Zein NPs and 78.29 ± 3.71% for empty NPs, corresponding to a final concentration of 4 mg mL^{-1} of zein in both nanoformulations. The encapsulation efficiency for Zein nanoparticles loaded with *S. montana* EO (EO-Zein NPs) was 20.58 ± 1.82%, which is equivalent to a final concentration of 1 mg of encapsulated EO per mL^{-1} of nanoformulation.

Particle physical stability was evaluated over 3 months by measuring size, PDI and surface charge (zeta-potential) when stored at 4 °C. The physical stability over time of EO-Zein NPs and Zein NPs are presented in Table 2.

Table 2. Stability, surface charge and polydespersion index of EO-Zein NPs and empty zein NPs, assessed with the dinamic light scattering method.

Sample	Time (Days)	Size (nm)	SD	PDI	SD	Zeta-Potential	SD
Zein NPs	0	142.3	4.88	0.222	0.025	30.3	1.01
	7	132.9	7.53	0.364	0.034	28.8	1.41
	30	122.7	11.87	0.361	0.024	28.9	0.451
	60	128.8	9.383	0.324	0.008	30.1	0.764
	90	122.1	7.804	0.261	0.02	29.8	2.04
EO-Zein NPs	0	159.1	3.99	0.338	0.108	30.3	1.13
	7	152.5	5.233	0.254	0.017	26.9	2.112
	30	149.3	3.782	0.232	0.003	28.3	2.4
	60	151.7	3.755	0.218	0.01	30.5	0.721
	90	150.5	3.922	0.211	0.007	30.1	0.764

The NPs remained stable through the 90 days of storage at 4 °C (last measurement), exhibiting along of these 90 days, sizes ranging between 122–160 nm. Both zein NPs with and without the *S. montana* EO, presented a monodisperse character and surface charge with approximately +30 mV, indicating that Zein produced uniform and stable particles.

3.2. Xeu Quantification and Disease Symptom Monitoring

Bacterial quantification revealed pathogen presence in all Xeu-inoculated groups. Results indicate that all treatments reduced significantly ($p < 0.05$) Xeu amount in infected plants, compared to the infected control (CBX). However, EO-zein NPs and zein NPs alone reduced bacterial amount by a 38 and 202-fold respectively, while plants treated with the EO presented a 1.6-fold reduction in bacterial levels (Figure 2).

Disease symptoms were recorded 12 days after Xeu inoculation, 10 days after treatments. No Bs symptoms were observed in uninoculated tomato leaves (CBC; CBS; CBSZ; CBZ) (Figure 3a–d). All infected plants, positive control (CBX) and treated plants (CBXS; CBXZ; CBXSZ) showed Bs symptoms characterized by necrotic/chlorotic leaf spots (Figure 3e,f). These results on leaf symptomatology are according to what was observed in bacterial quantification by q-PCR (Figure 2).

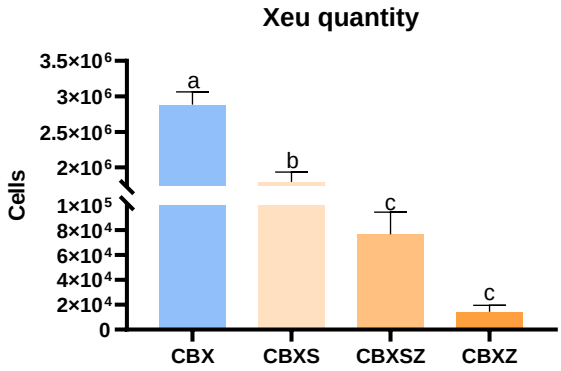

Figure 2. Comparison of *X. euvesicatoria* amount in infected tomato plants, quantified through qPCR. Values are presented as mean ± standard deviation (n = 3). Means marked with the same letter are not statistically different according to the Dunnett comparison test ($p < 0.05$). CBX-Infected + Untreated; CBXS-Infected + EO; CBXSZ-Infected + EO-zein NPs; CBXZ-Infected + Zein NPs.

Figure 3. Disease symptom monitoring, 12 days after infection (10 days after treatments). (**a**) Uninfected + Untreated (CBC, negative control); (**b**) Uninfected + EO (CBS); (**c**) Uninfected + EO-zein NPs (CBSZ); (**d**) Uninfected + Zein NPs (CBZ); (**e**) Infected + Untreated (CBX, positive control); (**f**) Infected + EO (CBXS); (**g**)-Infected + EO-zein NPs (CBXSZ); (**h**) Infected + Zein NPs (CBXZ).

3.3. ROS Quantification

The content on hydrogen peroxide was significantly ($p < 0.05$) increased by the application of the three treatments in uninfected plants (Figure 4a). Xeu infected plants showed a significant increase in both H_2O_2 and O_2^-, compared to the uninfected control (CBC) (Figure 4a,c). The application of *S. montana* EO (CBS), EO-zein NPs (CBSZ) and zein NPs (CBZ) led to a significant ($p < 0.05$) decrease in superoxide content (Figure 4c). When treatments were applied to Xeu infected plants, significant reductions in H_2O_2 and O_2^- were observed (Figure 4b,d).

3.4. Non-Enzymatic Antioxidant Capacity

The phenol content of tomato plants increased significantly ($p < 0.05$) in plants infected with Xeu (CBX) and in tomatoes treated with EO-zein NPs (CBSZ) and zein NPs (CBZ), compared to the uninfected control (CBC) (Figure 5a). No significant changes in the phenol content of infected plants were observed 10 days after the application of treatments (Figure 5b). The antiradical activity of leaf extracts increased significantly ($p < 0.05$) in Xeu infected plants (CBX) (Figure 5c). Furthermore, antiradical activity significantly decreased when *S. montana* EO (CBS), EO-zein NPs (CBSZ) and zein NPs (CBZ) were applied to uninfected plants (Figure 5c). Finally, 10 days after the application of treatments, the

antiradical activity of Xeu infected plants significantly decreased compared to the infected control (CBX) (Figure 5d).

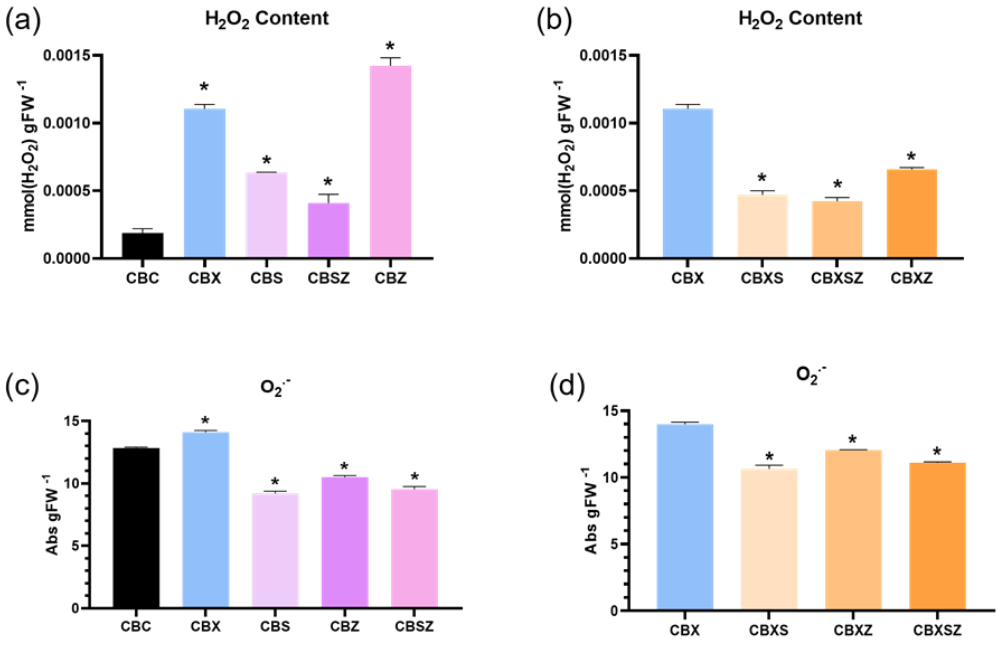

Figure 4. Hydrogen peroxide and superoxide radical content of tomato leaves 12 days after infection and 10 days after treatment application. (**a**,**c**) represent the levels of uninfected/treated groups (CBS; CBSZ; CBZ) and infected control (CBX) compared to the uninfected control (CBC). (**b**,**d**) represent the levels on infected/treated (CBXS; CBXSZ; CBXZ) groups compared to the infected/untreated control (CBX). Values are presented as mean ± standard deviation (n = 3). Means marked with an asterisk are statistically different from the respective control group according to the Dunnett comparison test ($p < 0.05$).

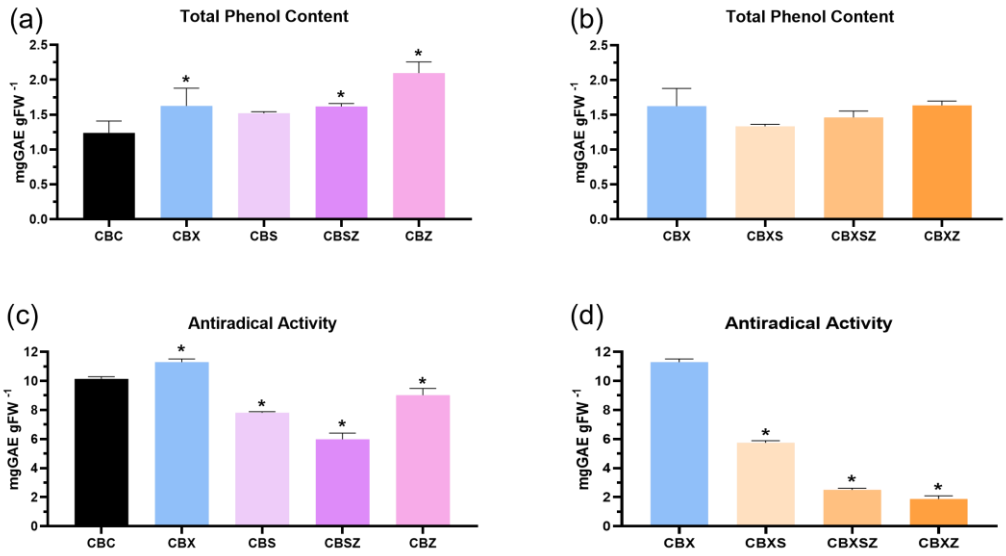

Figure 5. Total phenol content (**a**,**b**) and antiradical activity (**c**,**d**) of tomato leaves 12 days after *X. euvesicatoria* infection and 10 days after treatments. (**a**,**c**) represent the levels on uninfected/treated groups (CBS; CBSZ; CBZ) and infected/untreated control (CBX) compared to the uninfected/untreated control (CBC). (**b**,**d**) represent levels on infected/treated groups (CBXS; CBXSZ; CBXZ) compared to the infected/untreated control (CBX). Values are presented as mean ± standard deviation (n = 3). All means marked with an asterisk are statistically different of the respective control according to the Dunnett comparison test ($p < 0.05$).

3.5. Antioxidant Enzymatic Activity

Xeu infected plants presented a significant decrease in the TSP content 12 days after infection. TSP also increased significantly in plants treated with *S. montana* EO (CBS) and decreased significantly 10 days after the application of zein NPs (Figure 6a). The application of treatments to Xeu infected plants did not produce any significant changes in TSP content, compared to the infected control (CBX) (Figure 6b). Likewise, there were not significant differences in guaiacol peroxidase (GPX), catalase (CAT) and superoxide dismutase (SOD) activities in infected plants 10 days after treatments (Figure 6d,f,h). However, the application of zein NPs to uninfected plants significantly ($p < 0.05$) increased the activity of guaiacol peroxidase (GPX) (Figure 6c) and significantly decreased CAT activity. Concerning SOD activity, there were no differences when compared to infected or uninfected controls respectively (CBC; CBX) (Figure 6g,h).

3.6. Gene Expression

3.6.1. Phenylpropanoid Pathway

The application of the treatments to uninfected plants upregulated *crtiso*. Also, *crtiso* showed a significant upregulation ($p < 0.05$) in Xeu infected plants compared to the uninfected control (CBC) (Figure 7a). On the other hand, this gene was also upregulated by the application of EO-zein NPs in infected plants (CBXSZ) and downregulated by the application of *S. montana* EO and zein NPs, compared to Xeu infected plants (CBX) (Figure 7b). Concerning the phenylpropanoid pathway, *pal5* was significantly ($p < 0.05$) upregulated in Xeu infected plants, compared to the uninfected control (CBC). In plants treated with EO-zein NPs (CBSZ), an upregulation of *pal5* was observed, compared to CBC. EO-zein NPs also stimulated *pal5* 10 days after its application to Xeu infected plants (CBXSZ) (Figure 7b). Both *chs1* and *dfr* showed a significant upregulation when zein NPs were applied to uninfected tomato plants (Figure 7e,h). *chs1* was also upregulated by EO application in Xeu infected plants (CBXS) (Figure 7f). On the other hand, *dfr* was significantly ($p < 0.05$) upregulated by EO-zein NPs and zein NPs alone, in Xeu infected plants (CBXSZ and CBXZ respectively) (Figure 7h). Finally, 10 days after application, the treatments led to a downregulation of *fls*, compared to both uninfected and infected tomato plants (CBC and CBX respectively) (Figure 7i,j).

3.6.2. Enzymatic Pathway

Both *apxcyto* and *sod* were significantly ($p < 0.05$) upregulated in Xeu infected plants, compared to the uninfected control (CBC) (Figure 8a,c). The application of zein NPs also upregulated *apxcyto* and sod in uninfected plants (CBZ). On the other hand, *S. montana* EO upregulated sod 10 days after application (CBS) (Figure 8c), while EO-zein NPs upregulated *apxcyto* in uninfected plants (CBSZ) (Figure 8a). The application of zein NPs significantly ($p < 0.05$) upregulated *apxcyto* levels in Xeu infected plants (CBXZ) (Figure 8b). Treatments downregulated sod expression 10 days after application in Xeu infected plants (Figure 8d).

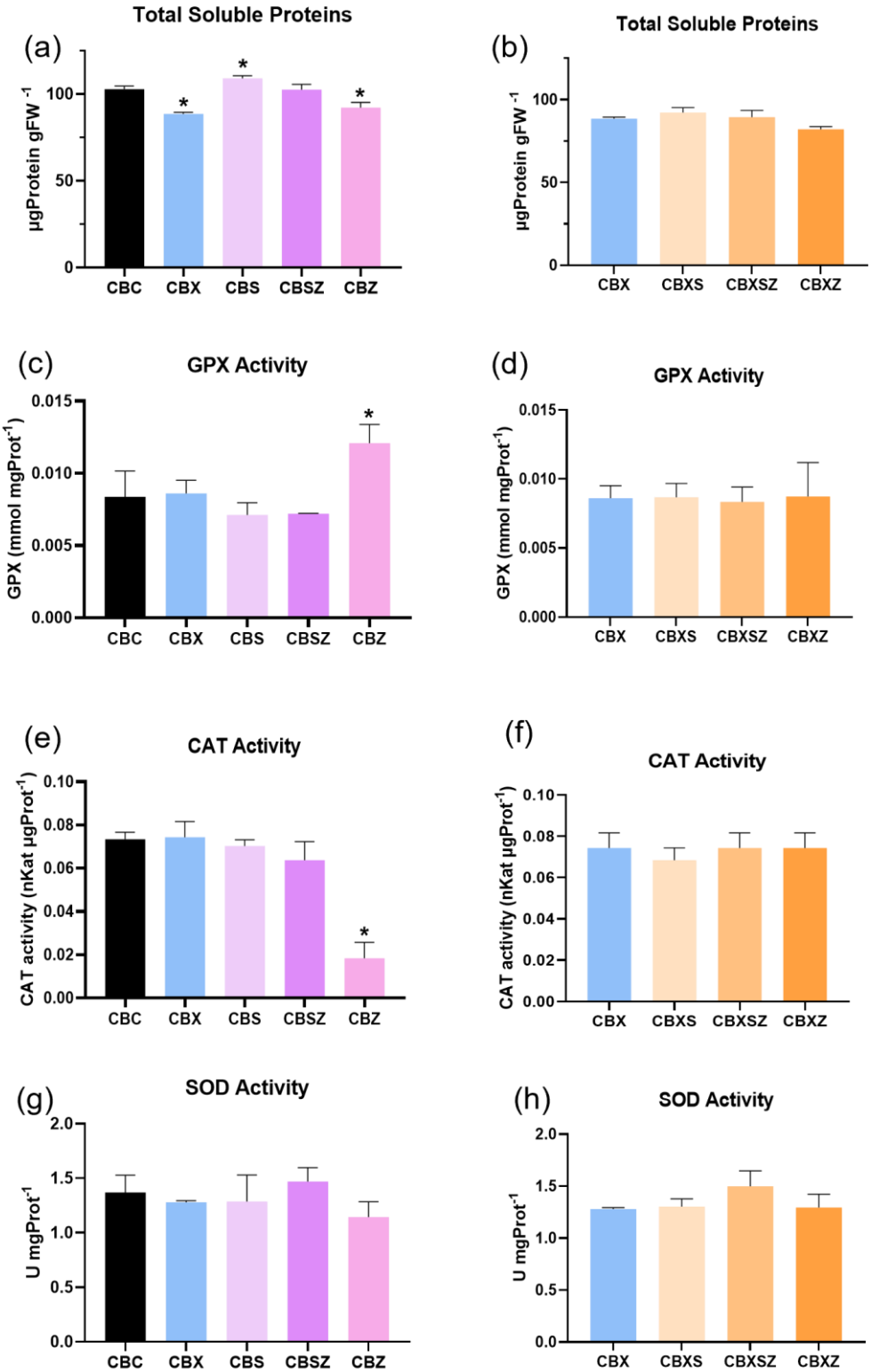

Figure 6. Effect of treatments (EO; EO-zein NPs; zein NPs) on tomato plants infected and uninfected with *X. euvesicatoria* 10 days after treatments. Total soluble protein content (**a**,**b**). GPX activity (**c**,**d**), CAT activity (**e**,**f**) and SOD activity (**g**,**h**). (**a**,**c**,**e**,**g**) represent the activities of uninfected/treated groups (CBS; CBSZ; CBZ) and the infected/untreated control (CBX) compared to the uninfected/untreated control (CBC). (**b**,**d**,**f**,**h**) epresent the activity levels of infected/treated groups (CBXS; CBXSZ; CBXZ) compared to the infected/untreated control (CBX). The values are presented as mean ± standard deviation (n = 3). Values marked with "*" are statistically different from the respective control according to the Dunnett comparison test ($p < 0.05$).

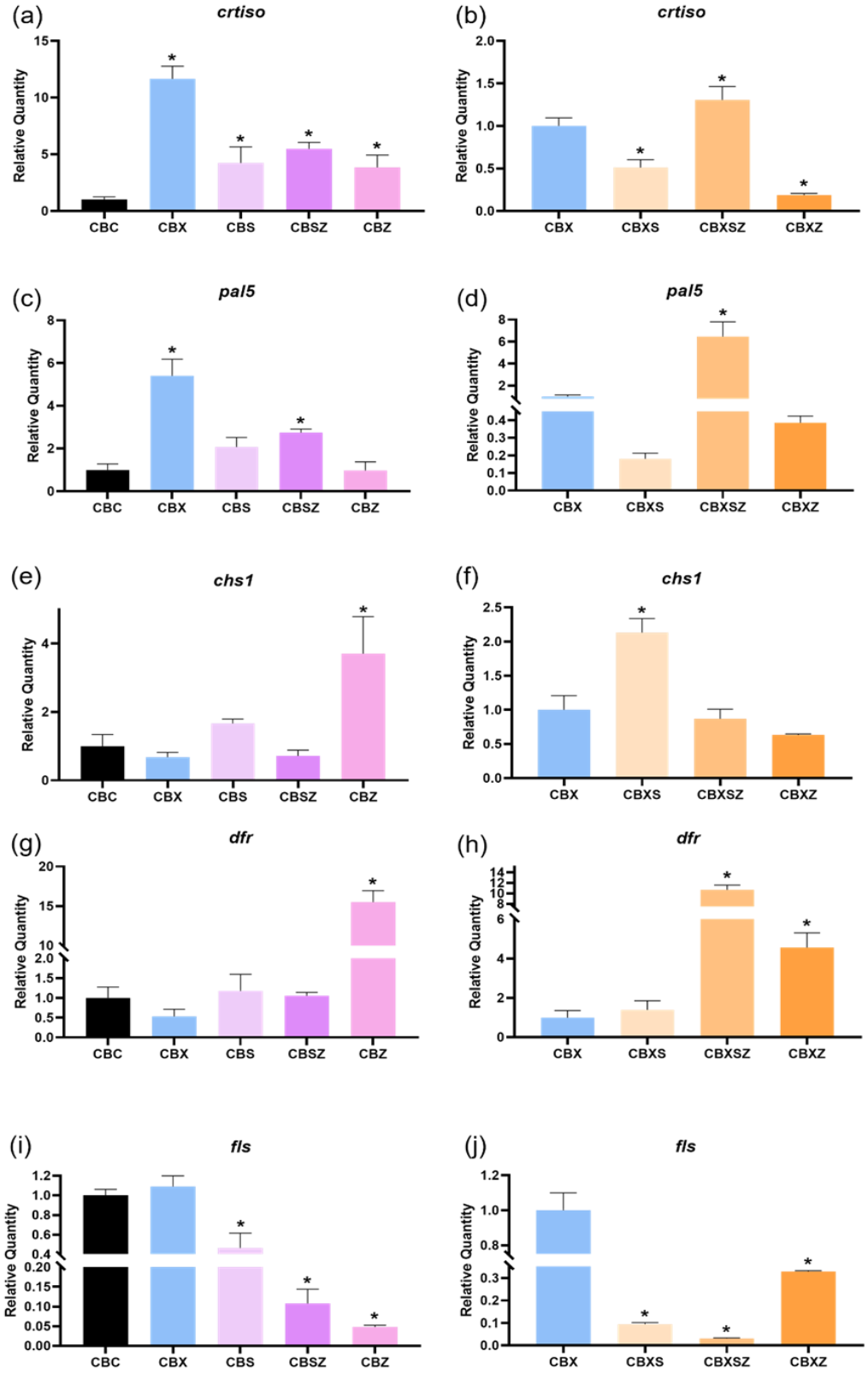

Figure 7. Expression levels of genes related to the carotenoid (*crtiso*) and phenylpropanoid (*pal5*; *chs1*; *dfr*; *fls*) pathways 10 days after treatments. Relative expression levels were determined by q-PCR. (**a**,**c**,**e**,**g**,**i**) represent the uninfected/treated groups (CBS; CBSZ; CBZ) and the infected/untreated control (CBX) normalized to the negative control (CBC). (**b**,**d**,**f**,**h**,**j**) represent the infected/treated groups (CBXS; CBXSZ; CBZ) compared to the positive control (CBX). Values are presented as mean ± standard deviation. All values marked with an asterisk are statistically different from the respective control following the Dunnett comparison test ($p < 0.05$).

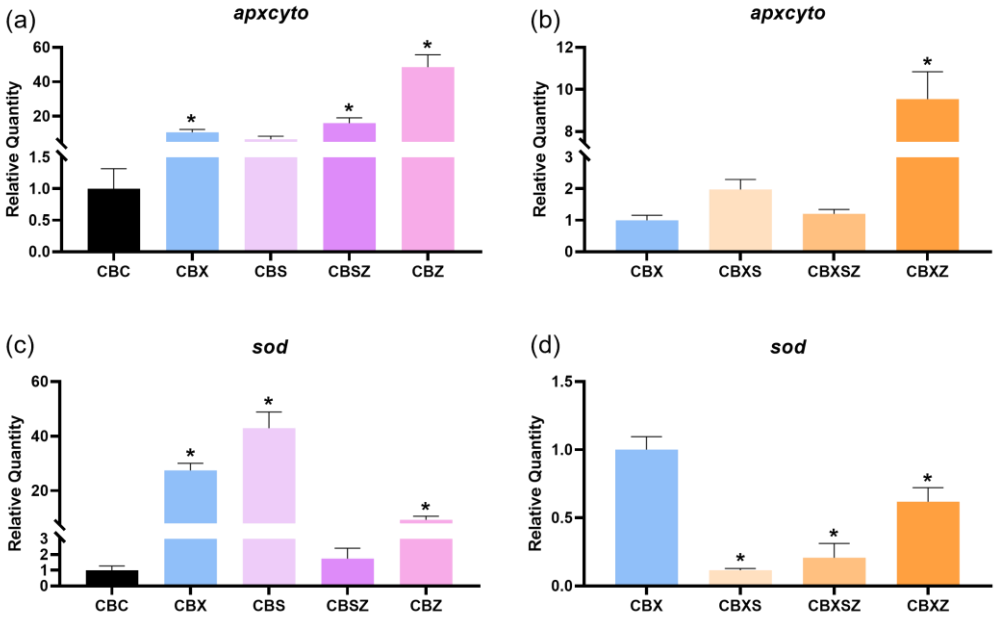

Figure 8. Relative expression levels of genes related to the antioxidant/enzymatic pathway, *apxcyto* (**a**,**b**) and *sod* (**c**,**d**) 10 days after treatments. Expression levels were determined by quantitative PCR. a and c stand for the uninfected/treated groups (CBS; CBSZ; CBZ) and the infected/untreated group (CBX) compared to the negative control (CBC). (**b**,**d**) represent the infected/treated groups (CBXS; CBXSZ; CBXZ) compared to the positive control (CBX). The values are presented as mean ± standard deviation, and all values marked with an asterisk are statistically different by the Dunnett comparison test ($p < 0.05$).

3.6.3. Hormone Pathway

Both ABA aldehyde oxidase (*aao*) and *opr3* showed a significant upregulation on Xeu infected plants, compared to the uninfected control (CBC) (Figure 9a,c). The application of *S. montana* EO also led to an upregulation of *aao* and *opr3* in uninfected tomato plants (CBS) (Figure 9a,c). *aao* was upregulated when EO-zein NPs were applied on uninfected plants (CBXSZ) (Figure 9a). The *aao* and *opr3* genes showed a significant ($p < 0.05$) downregulation 10 days after the application of EO and zein NPs on Xeu infected plants (CBXS and CBXSZ respectively) (Figure 9b,d). EO-zein NPs also downregulated *aao* expression levels in infected plants when compared to the infected control (CBX) (Figure 9b).

3.7. Principle Component Analysis

Principal component analysis showed a separation between tested groups, including the uninfected and infected controls (CBC and CBX respectively). PC1 explained 40% of the variance, and PC2 22% of the variance. Regarding the treatments on tomato plants infected with Xeu, CBXS and CBXZ were not significantly separated, and, among all treatments, these performed closer to the uninfected/untreated control (CBC). EO and zein (CBXSZ) was well separated from other conditions (upper left quadrant), showing a distinct impact of this treatment. All the treatments clearly changed the plants' phenotype when compared to the infected/untreated control (CBX).

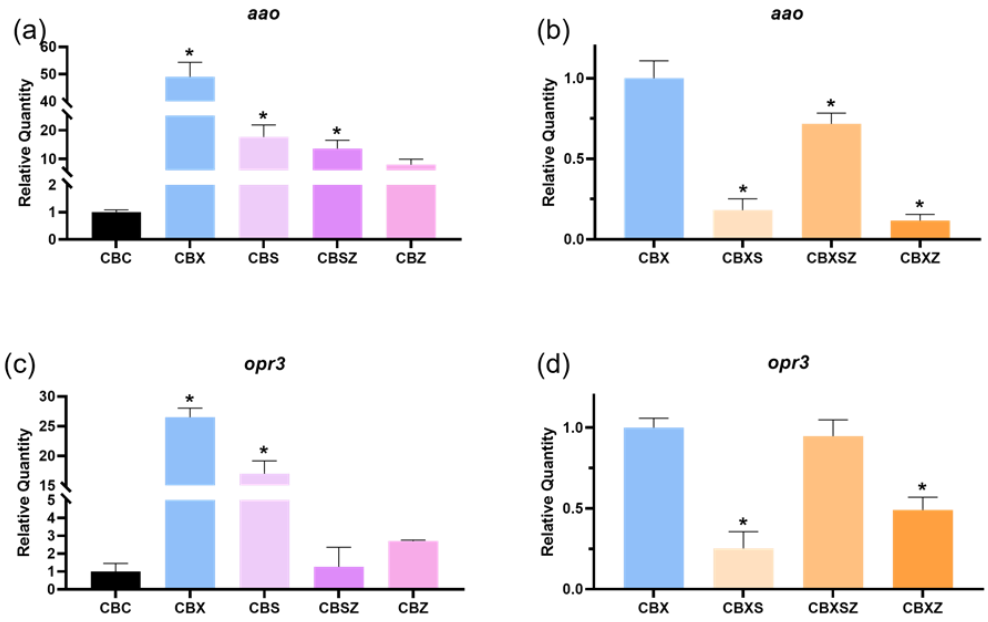

Figure 9. Relative expression levels of ABA and JA related pathways, *aao* (**a**,**b**) and *opr3* (**c**,**d**) respectively, 10 days after treatments. Expression levels were determined through q-PCR. (**a**,**c**)represent the uninfected/treated groups (CBS; CBSZ; CBZ) and the infected/untreated group (CBX) normalized to the negative control (CBC). While (**c**,**d**) stand for the infected/treated groups (CBXS; CBXSZ; CBXZ) compared with the positive control (CBX). Values are presented as mean ± standard deviation (n = 3). All values marked with "*" are statistically different from the control, according to the Dunnett comparison test ($p < 0.05$).

4. Discussion

S. lycopersicum is threatened by several bacterial diseases, among which Bs presents a major concern. Current control methods for bacterial diseases in plant production are predominantly based on Cu-based products, but bacterial pathogens showing resistance to Cu are increasingly being found. European governments have applied some strategies toward the improvement of organic farming by developing alternatives for plant protection. Therefore, organic products like EOs (alone or stabilized/carried in NP-based nanoformulations) could fill this gap since they are extracted from plants, biodegradable, and economically viable [56]. *Satureja* EOs are known to have antimicrobial properties against several plant pathogens and have already shown effectiveness against some *Xanthomonas* sp. [32]. However, *Satureja montana* EO was not reported as an effective control agent of *X. euvesicatoria* until now.

In this work we explored the *S. montana* EO, free or encapsulated in zein NPs, and empty zein NPs as new agents for the treatment and control of *X. euvesicatoria* in tomato. Some variations on zein NPs and EO-Zein NPs mean size, PDI and surface charge (zeta-potential) were detected during storage (Table 2). These variations are most likely related with rearrangements of zein protein at the NP surface [57]. However, these variations were not significant and did not affect the NPs' stability and physical properties. An increase in NP size was noticeable when comparing EO loaded NPs with empty ones. This increase in nanoparticles' size might be related with the encapsulation of the *S. montana* EO. This phenomenon was already described when encapsulating other EOs in zein NPs [58]. The encapsulating efficiency was also within the values previously reported for other essential oils when encapsulated in zein-based nanoparticles [58].

The data presented here suggest that the application of EO unequivocally reduces the Xeu load on tomato plants as previously reported for *S. hortensis* EO in *X. axanopodis* [32]. However, the effect of the EO on the reduction of the amount of bacteria was clearly improved by its encapsulation in zein NPs (Figure 3). These findings are supported by

Poyatos-Racionero et al. [59], who reported that zein enhances the antimicrobial activity of EOs by decreasing their volatility. These data also show that zein NPs alone presented high antimicrobial activity. It should be noted that, despite being reported as effective carriers of EOs and other antimicrobial compounds [60–62], some works also report that zein itself possesses antimicrobial properties [63]. However, to our knowledge this is the first report suggesting that zein NPs possess antimicrobial activity against phytopathogens, namely Xeu. Zein nanoparticles have been extensively studied for their coating properties, which make them suitable for drug delivery and have been considered "generally regarded as safe" for oral pharmaceuticals by the FDA [64]. Nevertheless, their capability to act as antimicrobial agents against plant bacterial diseases remain unexplored. These results widen the scope for zein as a protein of interest in the agricultural field, not only as a drug delivery tool but also as a plant-based protein with antimicrobial activity.

The reduction of Xeu amount in EO-treated plants (Figure 2) may be due to the EO composition. Some of the EO's compounds (e.g., thymol and carvacrol) have known antioxidant and antimicrobial capacities [37,61,65]. These biomolecules may act directly as antimicrobials or elicit the plant's defenses against pathogens [66]. Also, the zein treated plants showed a decrease in Xeu amount, supporting previous reports on the zein protein possessing antimicrobial properties [63]. Therefore, the reduction of ROS content in tomato leaves (Figure 4) might be due to these products' protective role on plant cell mechanisms, allied with their antimicrobial activity (Figure 2). The results clearly demonstrate that they have an antioxidant activity on tomato leaves by reducing the hydrogen peroxide and superoxide radical levels (Figure 4b,d). Associated with these products' antimicrobial activity (Figure 2), ROS levels remain at low concentrations, since high levels of ROS play a major role in plants' defense systems against bacterial pathogens [67]. This hypothesis is supported on the fact that the infected control (CBX) presented a higher level of both H_2O_2 and O_2^- (Figure 4) than uninfected control plants (CBC) demonstrating the pivotal role of ROS in plants' defense as reported previously [68]. The reduction in ROS levels may have occurred through non-enzymatic mechanisms, namely by the accumulation of phenolic compounds (Figure 5) as verified in uninfected plants, where EO/zein treatments stimulated phenolic contents. On other hand, treatments in Xeu infected plants improved the antioxidant activity compared to CBX, which is aligned with the reduction of Xeu amount (Figure 2), showing that mitigation of the Bs disease may be promoted by EO and NP eliciting plant's defenses in uninfected plants, namely the phenylpropanoid pathway. However, the anti-radical activity, assessed through the DPPH-scavenging activity was significantly reduced by treatments in infected plants (Figure 5d). Enzymatic activities are apparently not stimulated by Xeu infection nor treatments, except for CBZ that promotes an increase of the group of peroxidases using guaiacol (Figure 4). Despite the little effect on the GPX activity, our data show that both EO and zein overregulate *apx* and *sod* expression in uninfected plants, (Figure 6), and downregulate *sod* expression in infected plants compared to CBX. These data may indicate that the EO and/or zein activate the pool of these enzymes' transcripts, which may improve tomato's resilience against Bs disease. The antioxidant enzymatic pathways have been already referred to as an important mechanism of tomato resistance to Bs disease [69,70].

Complementary to the enzymatic pathways, tomato plants under pathogenic bacterial infection, e.g., *Ralstonia solanacearum*, have increased levels of non-enzymatic antioxidant metabolites in leaves, which helps to prevent major impacts from the pathogenic attack [71]. Thus, some antioxidant pathways were stimulated by our treatments. This stimulus remained 10-days after application in infected and uninfected plants. This may indicate that zein and *S. montana* EO improve plant's resistance to Bs and reduce Xeu amount through the upregulation of the phenylpropanoid and carotenoid pathways. Then, the significant increase in *crtiso* transcripts during Xeu infection (CBX) indicates that the lycopene pathway plays a major role in tomatoes' defense against Xeu. The upregulation of *crtiso* may be associated with high levels of ABA, once this plant hormone is reported to be at high levels during pathogen infection and to play a pivotal role on the regulation of plant

defense [72], including the upregulation of phenylpropanoid pathway [73]. When present at high concentrations in plant leaves, ABA is known to antagonize JA levels and inhibit the accumulation of phenylpropanoids and other defense compounds in plant leaves [74,75]. Also, as the *aao* gene was upregulated by Xeu infection, it may indicate a possible link to the role of ABA on plant immunity against Xeu, via lycopene pathway.

Results show a similar effect of EO and zein, increasing the transcript levels of those antioxidant pathways, related to the carotenoid pathway and also in the phenylpropanoid synthesis, except for the regulation of flavonols (*fls*). These results are in line with the increment of the *aao* transcript levels in Xeu-infected plants (CBX), EO treated uninfected plants (CBS) and EO-zein NPs treated uninfected plants (CBSZ) (Figure 9). This stimulus, in particular for zein application, on phenylpropanoid pathway, namely related to anthocyanins synthesis in leaves, may suggest that the flavanol pathway might not play a major role in tomatoes' defense response against Xeu. Our data further show that treatments were able to reduce *aao* levels in infected plants, indicating a reduction in ABA which is important to plants' defense against biotic stress. The *opr3* levels were upregulated in Xeu infected plants (CBX) and in EO treated uninfected plants, suggesting the capacity of *S. montana* EO to activate plants' defense even in the absence of a bacterial threat (Figure 9), and consequently supporting its potential as a prophylactic agent. EO and zein NPs treatments also led to a downregulation of *opr3* in Xeu infected plants (Figure 9d) which might be due to the better health status of treated plants, corroborated by Xeu load reduction (Figure 2) and apparently improved health status (Figure 3) of treated plants. Whole data analysis integrated by PCA distribution (Figure 10) indicates a different plant behavior with the absence/presence of Xeu infection. Besides that, the separated application of EO and zein promotes an identical response in the plant resistance against Bs disease. Nevertheless, a synergic protective effect of EO-zein NPs changed the plant's health status, separating treated plants from the uninfected/untreated control (CBC). This may be due to a long-term protective effect (improved immunity), supported here by the increase on transcripts of the phenylpropanoid pathway, namely *crtiso*, *pal5* and *dfr*. This protective role from the phenylpropanoid pathway in tomato plants against disease has been already reported [76,77].

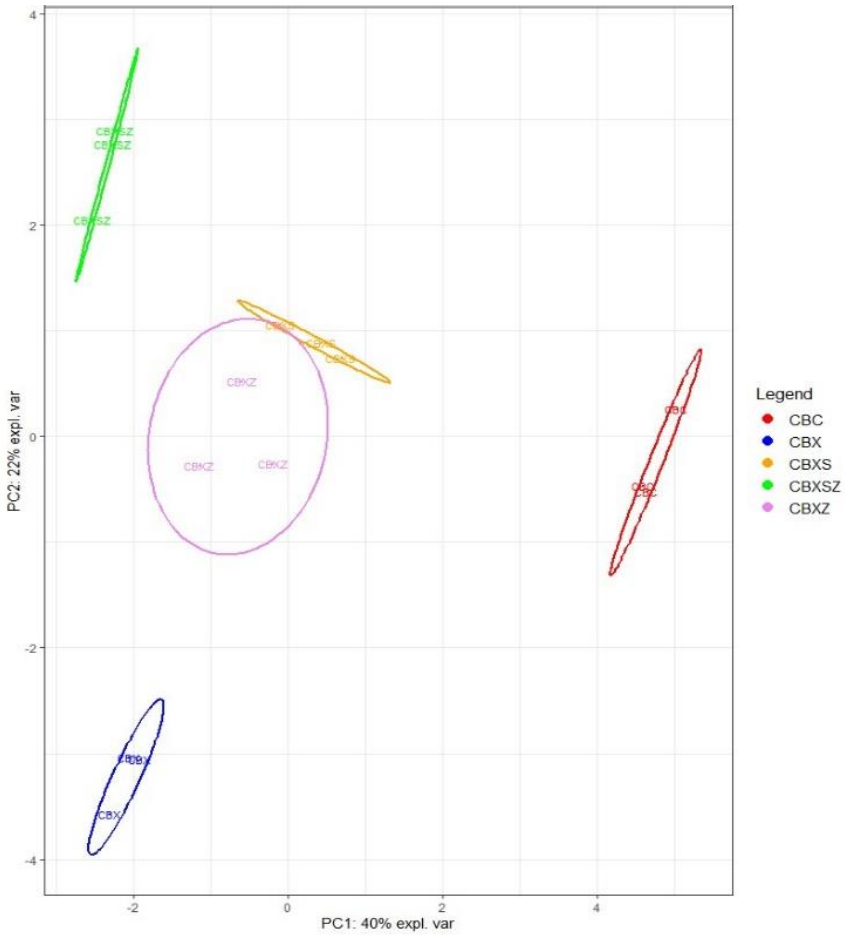

Figure 10. Principal component analysis (PCA) biplot with ellipses (confidence interval of 0.95) showing the effect of *S. montana* EO, EO-Zein NP nanoformulation and empty zein NPs on infected tomato plants. PC1 (first axis) explained 40% of the variance, while the PC2 (second axis) explained 22% of the variance. CBC—Uninfected/Untreated; CBX—Infected/Untreated; CBXS—Infected/EO; CBXSZ—Infected/EO-Zein NPs; CBXZ—Infected/Zein NPs.

5. Conclusions

S. montana EO, zein NPs and EO-zein NPs present antimicrobial activity against Xeu causing Bs of tomato *in planta*. Such effect ultimately leads to an improvement in plants' health, compared to infected ones (CBX). All three treatments seem equally effective on disease control, however zein NPs seem to modulate molecular pathways in uninfected plants (CBZ) suggesting a possible application as a prophylactic. Overall, our results indicate that *S. montana* EO, zein NPs and their combination could be effectively employed to control Bs caused by *X. euvesicatoria* in tomato orchards. This work is the first approach to the effect of *S. montana* EO against Xeu in tomato and its action when encapsulated in zein NPs. This is also the first study to assess and demonstrate the antimicrobial activity of zein NPs *in planta* as well as its effect in plants' stress related molecular pathways. Field studies are required to assess large scale in field implementation of this natural solution as well as its' potential as a disease prevention tool. Meanwhile the potential effect of the application of these compounds in the organoleptic properties of fruits should also be addressed. Data also suggest that the protective role of these products, as inferred by the accumulation of transcripts of some antioxidant-enzymes, deserves further studies.

Author Contributions: P.R.O.-P., N.M.-P., R.M.O.F.S., M.F.-F. and C.S. designed these experiments. Nanoformulations were developed by A.R. and A.C.-P. Tomato culture and *X. euvesicatoria* infection were performed by R.M.O.F.S. and A.T. with support from P.R.O.-P., N.M-P. and F.T. All plant assays

and bacterial quantification were performed by P.R.O.-P., supported by N.M-P. Data analysis was performed by P.R.O.-P. and N.M.-P. The manuscript was written by P.R.O.-P. with support from N.M.-P. All authors have read and agreed to the published version of the manuscript.

Funding: This work and APC were funded by the Portuguese Foundation for Science and Technology (FCT) through the LAQV-REQUIMTE Research Unit (UIDB/QUI/50006/2020).

Institutional Review Board Statement: The authors will make the results available, if requested.

Acknowledgments: The authors would like to thank other funding sources that supported the researchers involved in this work, such as, the European Investment Funds through the COMPETE 2020—Operational Programme for Competitiveness and Internationalization (POCI) and National Funds by the Portuguese Foundation for Science and Technology (FCT) (02/SAICT/2017, Ref. PTDC/BAAAGR/31131/2017, Acronym EOIS-CropProt). National Funds through FCT (Portugal) also funded this work within the scope of GreenUPorto, FCUP research unit: UIDB/05748/2020 and UIDP/05748/2020 projects; CITAB research unit, UTAD: project UIDB/04033/2020). Furthermore, N.M-P. was funded by a PhD grant SFRH/BD/138187/2018. This study was also supported by the European Union's Horizon 2020 Research and Innovation Program (Grant Agreement Number 857251).

Conflicts of Interest: The authors declare no conflict of interest.

References

1. Guan, Z.; Biswas, T.; Wu, F. *The US Tomato Industry: An Overview of Production and Trade: FE1027, 9/2017*, 1st ed.; EDIS: Gainesville, FL, USA, 2018.
2. Horvath, D.M.; Stall, R.E.; Jones, J.B.; Pauly, M.H.; Vallad, G.E.; Dahlbeck, D.; Staskawicz, B.J.; Scott, J.W. Transgenic resistance confers effective field level control of bacterial spot disease in tomato. *PLoS ONE* **2012**, *7*, e42036. [CrossRef]
3. Potnis, N.; Timilsina, S.; Strayer, A.; Shantharaj, D.; Barak, J.D.; Paret, M.L.; Vallad, G.E.; Jones, J.B. Bacterial spot of tomato and pepper: Diverse *Xanthomonas* species with a wide variety of virulence factors posing a worldwide challenge. *Mol. Plant Pathol.* **2015**, *16*, 907–920. [CrossRef] [PubMed]
4. Jones, J.B.; Bouzar, H.; Stall, R.E.; Amlira, E.C.; Roberts, P.D.; Bowen, B.W.; Sudberry, J.; Strickler, P.M.; Chun, J. Systematic analysis of Xanthomonads (*Xanthomonas* spp.) associated with pepper and tomato lesions. *Intl. J. Syst. Evol. Microbiol.* **2000**, *50*, 1211–1219. [CrossRef] [PubMed]
5. Egel, D.S.; Jones, J.B.; Minsavage, G.V.; Creswell, T.; Ruhl, G.; Maynard, E.; Marchino, C. Distribution and characterization of *Xanthomonas* strains causing bacterial spot of tomato in Indiana. *Plant Health Prog.* **2018**, *19*, 319–321. [CrossRef]
6. Itako, A.T.; Tolentino, J.B.; Silva, T.A.F.D.; Soman, J.M.; Maringoni, A.C. Chemical products induce resistance to *Xanthomonas perforans* in tomato. *Braz. J. Microbiol.* **2015**, *46*, 701–706. [CrossRef]
7. Liao, Y.Y.; Strayer-Scherer, A.L.; White, J.; Mukherjee, A.; De La Torre-Roche, R.; Ritchie, L.; Colee, J.; Vallad, G.E.; Freeman, J.H.; Jones, J.B.; et al. Nano-Magnesium oxide: A novel bactericide against copper-tolerant *Xanthomonas perforans* causing tomato bacterial spot. *Phytopathology* **2019**, *109*, 52–62. [CrossRef]
8. Liu, Q.; Zhang, S.; Huang, Y.; Jones, J.B. Evaluation of a small molecule compound 3-indolylacetonitrile for control of bacterial spot on tomato. *Crop Prot.* **2019**, *120*, 7–12. [CrossRef]
9. Vallad, G.E.; Pernezny, K.L.; Balogh, B.; Wen, A.; Figueiredo, J.F.L.; Jones, J.B.; Momol, T.; Muchovej, R.M.; Havranek, N.; Abdallah, N.; et al. Comparison of kasugamycin to traditional bactericides for the management of bacterial spot on tomato. *HortScience* **2010**, *45*, 1834–1840. [CrossRef]
10. Strayer-Scherer, A.; Liao, Y.Y.; Abrahamian, P.; Timilsina, S.; Paret, M.; Momol, T.; Jones, J.; Vallad, G.E. *Integrated Management of Bacterial Spot on Tomato in Florida*, 1st ed.; EDIS: Gainesville, FL, USA, 2019; p. 8. [CrossRef]
11. Jamiołkowska, A. Natural compounds as elicitors of plant resistance against diseases and new biocontrol strategies. *Agronomy* **2020**, *10*, 173. [CrossRef]
12. Arasu, M.V.; Al-Dhabi, N.A.; Choi, K.C.; Bensy, A.D.V.; Rajaselvam, J. Bioactive potential of *Albizia lebbeck* extract against phytopathogens and protective properties on tomato plant against speck disease in greenhouse. *Physiol. Mol. Plant Pathol.* **2021**, *117*, 101750. [CrossRef]
13. Liberto, M.G.D.; Seimandi, G.M.; Fernández, L.N.; Ruiz, V.E.; Svetaz, L.A.; Derita, M.G. Botanical Control of Citrus Green Mold and Peach Bro wn Rot on Fruits Assays Using a *Persicaria acuminata* Phytochemically Characterized Extract. *Plants* **2021**, *10*, 425. [CrossRef] [PubMed]
14. Tamm, L.; Thürig, B.; Fliessbach, A.; Goltlieb, A.E.; Karavani, S.; Cohen, Y. Elicitors and soil management to induce resistance against fungal plant diseases. *NJAS Wagening. J. Life Sci.* **2011**, *58*, 131–137. [CrossRef]
15. Burketova, L.; Trda, L.; Ott, P.G.; Valentova, O. Bio-based resistance inducers for sustainable plant protection against pathogens. *Biotechnol. Adv.* **2015**, *33*, 994–1004. [CrossRef] [PubMed]
16. Bajpai, V.K.; Kang, S.R.; Xu, H.; Lee, S.G.; Baek, K.H.; Kang, S.C. Potential roles of essential oils on controlling plant pathogenic bacteria *Xanthomonas* species: A review. *Plant Pathol. J.* **2011**, *27*, 207–224. [CrossRef]

17. Pepa, T.D.; Elshafie, H.S.; Capasso, R.; De Feo, V.; Camele, I.; Nazzaro, F.; Scognamiglio, M.R.; Caputo, L. Antimicrobial and phytotoxic activity of *Origanum heracleoticum* and *O. majorana* essential oils growing in Cilento (Southern Italy). *Molecules* **2019**, *24*, 2576. [CrossRef] [PubMed]
18. Alkan, D.; Yemenicioğlu, A. Potential application of natural phenolic antimicrobials and edible film technology against bacterial plant pathogens. *Food Hydrocoll.* **2016**, *55*, 1–10. [CrossRef]
19. Abo-Elyousr, K.A.; Bagy, H.M.K.; Hashem, M.; Alamri, S.A.; Mostafa, Y.S. Biological control of the tomato wilt caused by *Clavibacter michiganensis* subsp. *michiganensis* using formulated plant growth-promoting bacteria. *Egypt. J. Biol. Pest Control* **2019**, *29*, 54. [CrossRef]
20. Franz, C.; Novak, J. Sources of essential oils. In *Handbook of Essential Oils*; Baser, K.H.C., Buchbauer, G., Eds.; CRC Press: Boca Raton, FL, USA, 2020; pp. 41–83.
21. Mollova, S.; Fidan, H.; Antonova, D.; Bozhilov, D.; Stanev, S.; Kostova, I.; Stoyanova, A. Chemical composition and antimicrobial and antioxidant activity of *Helichrysum italicum* (Roth) G. *Don subspecies essential oils. Turk. J. Agric. For.* **2020**, *44*, 371–378. [CrossRef]
22. Magi, G.; Marini, E.; Facinelli, B. Antimicrobial activity of essential oils and carvacrol, and synergy of carvacrol and erythromycin, against clinical, erythromycin-resistant Group A Streptococci. *Front. Microbiol.* **2015**, *6*, 165. [CrossRef] [PubMed]
23. Chouhan, S.; Sharma, K.; Guleria, S. Antimicrobial activity of some essential oils—Present status and future perspectives. *Medicines* **2017**, *4*, 58. [CrossRef]
24. Guo, F.; Chen, Q.; Liang, Q.; Zhang, M.; Chen, W.; Chen, H.; Yun, Y.; Zhong, Q.; Chen, W. Antimicrobial Activity and Proposed Action Mechanism of Linalool against *Pseudomonas fluorescens*. *Front. Microbiol.* **2021**, *12*, 49. [CrossRef]
25. Bajpai, V.K.; Cho, M.J.; Kang, S.C. Control of plant pathogenic bacteria of *Xanthomonas* spp. by the essential oil and extracts of *Metasequoia glyptostroboides* Miki ex Hu In Vitro and In Vivo. *J. Phytopathol.* **2010**, *158*, 479–486. [CrossRef]
26. Altundag, S.; Aslim, B.E.L.M.A.; Ozturk, S. In Vitro Antimicrobial Activities of Essential Oils from *Origanum minutiflorum* and *Sideritis erytrantha* subsp. *erytrantha* on Phytopathogenic Bacteria. *J. Essent. Oil Res.* **2011**, *23*, 4–8. [CrossRef]
27. Costa, P.; Medronho, B.; Goncalves, S.; Romano, A. Cyclodextrins enhance the antioxidant activity of essential oil. *Ind. Crop. Prod.* **2015**, *70*, 341–346. [CrossRef]
28. Cunha, A.P.; Ribeiro, J.A.; Roque, O.R. *Plantas Aromáticas em Portugal. Caracterização e Utilizações*, 1st ed.; Fundação Calouste Gulbenkian: Lisbon, Portugal, 2007.
29. Maccelli, A.; Vitanza, L.; Imbriano, A.; Frascetti, C.; Filippi, A.; Goldoni, P.; Maurizi, L.; Ammendolia, M.G.; Crestoni, M.E.; Fornarini, S.; et al. *Satureja montana* L. essential oil/chemical profiles/phitochemical screening, antimicrobial activity and O/W nanoemulsion formulations. *Pharmaceutics* **2020**, *12*, 7. [CrossRef] [PubMed]
30. Vitanza, L.; Maccelli, A.; Marazzato, M.; Scazzocchio, F.; Comanducci, A.; Fornarini, A.; Crestoni, M.E.; Filippi, A.; Frascetti, C.; Rinaldi, F.; et al. *Satureja montana* L. essential oil and its activity alone or in combination with gentamicin. *Microb. Pathog.* **2018**, *126*, 323–331. [CrossRef]
31. García-Díaz, M.; Gil-Serna, J.; Patiño, B.; García-Cela, E.; Magan, N.; Medina, A. Assessment of the effect of *Satureja montana* and *Organum virens* essential oils on *Aspergillus flavus* growth and aflatoxin production at different water activities. *Toxins* **2020**, *12*, 142. [CrossRef]
32. Kotan, R.; Dadasoğlu, F.; Karagoz, K.; Cakir, A.; Ozer, H.; Kordali, S.; Cakmakci, R.; Dikbas, N. Antibacterial activity of the essential oil and extracts of *Satureja hortensis* against plant pathogenic bacteria and their potential use as seed disinfectants. *Sci. Hortic.* **2013**, *153*, 34–41. [CrossRef]
33. Maurya, A.K.; Sharma, A.; Kumar, K.; Chander, R.; Kumar, A.; Kumar, D.; Padwad, Y.S.; Chand, G.; Agnihotri, V.K. Comparative studies of essential oils composition and cytotoxic activity of *Valeriana jatamansi* Jones. *J. Essent. Oil Res.* **2021**, 1–8. [CrossRef]
34. Wang, H.; Zhu, W.; Huang, Y.; Li, Z.; Jiang, Y.; Xie, Q. Facile encapsulation of hydroxycamptothecin nanocrystals into zein-based nanocomplexes for active targeting in drug delivery and cell imaging. *Acta Biomater.* **2017**, *61*, 88–100. [CrossRef]
35. Patel, A.; Hu, Y.; Tiwari, J.K.; Velikov, K.P. Synthesis and characterisation of zein–curcumin colloidal particles. *Soft Matter* **2010**, *6*, 6192–6199. [CrossRef]
36. Paliwal, R.; Palakurthi, S. Zein in controlled drug delivery and tissue engineering. *J. Control. Release* **2014**, *189*, 108–122. [CrossRef] [PubMed]
37. Bidyarani, N.; Srivastav, A.K.; Gupta, S.K.; Kumar, U. Synthesis and physicochemical characterization of rhamnolipid-stabilized carvacrol-loaded zein nanoparticles for antimicrobial application supported by molecular docking. *J. Nanoparticle Res.* **2020**, *22*, 307. [CrossRef]
38. Yilmaz, M.T.; Akman, P.K.; Bozkurt, F.; Karasu, S. An effective polydopamine coating to improve stability and bioactivity of carvacrol-loaded zein nanoparticles. *Int. J. Food Sci. Technol.* **2021**, *56*, 6011–6024. [CrossRef]
39. Merino, N.; Berdejo, D.; Bento, R.; Salman, H.; Lanz, M.; Maggi, F.; Sánchez-Gómez, S.; García-Gonzaloa, D.; Pagán, R. Antimicrobial efficacy of *Thymbra capitata* (L.) Cav. essential oil loaded in self-assembled zein nanoparticles in combination with heat. *Ind. Crop. Prod.* **2019**, *133*, 98–104. [CrossRef]
40. Monteiro, R.A.; Camara, M.C.; de Oliveira, J.L.; Campos, E.V.R.; Carvalho, L.B.; de Freitas Proença, P.L.; Guilger-Casagrande, M.; Lima, R.; do Nascimento, J.; Gonçalves, K.C.; et al. Zein based-nanoparticles loaded botanical pesticides in pest control: An enzyme stimuli-responsive approach aiming sustainable agriculture. *J. Hazard. Mater.* **2021**, *417*, 126004. [CrossRef]

41. Matsuda, Y.; Suzuki, T.; Sato, E.; Sato, M.; Koizumi, S.; Unno, K.; Kato, T.; Nakai, K. Novel preparation of zein microspheres conjugated with PS-K available for cancer immunotherapy. *Chem. Pharm. Bull.* **1989**, *37*, 757–759. [CrossRef]
42. Moretti, C.; Amatulli, M.T.; Buonaurio, R. PCR-based assay for the detection of *Xanthomonas euvesicatoria* causing pepper and tomato bacterial spot. *Lett. Appl. Microbiol.* **2009**, *49*, 466–471. [CrossRef]
43. Zhao, S.; Fernald, R.D. Comprehensive algorithm for quantitative real-time polymerase chain reaction. *J. Comput. Biol.* **2005**, *12*, 1047–1064. [CrossRef]
44. Alexieva, V.; Sergiev, I.; Mapelli, S.; Karanov, E. The effect of drought and ultraviolet radiation on growth and stress markers in pea and wheat. *Plant Cell Environ.* **2001**, *24*, 1337–1344. [CrossRef]
45. Gajewska, E.; Sklodowska, M. Effect of nickel on ROS content and antioxidative enzyme activities in wheat leaves. *BioMetals* **2007**, *20*, 27–36. [CrossRef]
46. Costa-Santos, M.; Mariz-Ponte, N.; Dias, M.C.; Moura, L.; Marques, G.; Santos, C. Effect of *Bacillus* spp. and *Brevibacillus* sp. on the Photosynthesis and Redox Status of *Solanum lycopersicum*. *Horticulturae* **2021**, *7*, 24. [CrossRef]
47. Dewanto, V.; Wu, X.; Adom, K.K.; Liu, R.H. Thermal processing enhances the nutritional value of tomatoes by increasing total antioxidant activity. *J. Agric. Food Chem.* **2002**, *50*, 3010–3014. [CrossRef]
48. Harkat-Madouri, L.; Asma, B.; Madani, K.; Said, Z.B.O.S.; Rigou, P.; Grenier, D.; Allalou, H.; Remini, H.; Adjaoud, A.; Boulekbache-Makhlouf, L. Chemical composition, antibacterial and antioxidant activities of essential oil of *Eucalyptus globulus* from Algeria. *Ind. Crop. Prod.* **2015**, *78*, 148–153. [CrossRef]
49. Mariz-Ponte, N.; Mendes, R.J.; Sario, S.; Melo, P.; Santos, C. Moderate UV-A supplementation benefits tomato seed and seedling invigoration: A contribution to the use of UV in seed technology. *Sci. Hortic.* **2018**, *235*, 357–366. [CrossRef]
50. Bradford, M.M. A rapid and sensitive method for the quantitation of microgram quantities of protein utilizing the principle of protein-dye binding. *Anal. Biochem.* **1976**, *72*, 248–254. [CrossRef]
51. Løvdal, T.; Lillo, C. Reference gene selection for quantitative real-time PCR normalization in tomato subjected to nitrogen, cold, and light stress. *Anal. Biochem.* **2009**, *387*, 238–242. [CrossRef] [PubMed]
52. Mariz-Ponte, N.; Mendes, R.J.; Sario, S.; De Oliveira, J.F.; Melo, P.; Santos, C. Tomato plants use non-enzymatic antioxidant pathways to cope with moderate UV-A/B irradiation: A contribution to the use of UV-A/B in horticulture. *J. Plant Physiol.* **2018**, *221*, 32–42. [CrossRef]
53. Murshed, R.; Lopez-Lauri, F.; Sallanon, H. Effect of water stress on antioxidant systems and oxidative parameters in fruits of tomato (*Solanum lycopersicon* L, cv. Micro-tom). *Physiol. Mol. Biol. Plants* **2013**, *19*, 363–378. [CrossRef] [PubMed]
54. Horváth, E.; Csiszár, J.; Gallé, Á.; Poór, P.; Szepesi, Á.; Tari, I. Hardening with salicylic acid induces concentration-dependent changes in abscisic acid biosynthesis of tomato under salt stress. *J. Plant Physiol.* **2015**, *183*, 54–63. [CrossRef]
55. Niwa, T.; Suzuki, T.; Takebayashi, Y.; Ishiguro, R.; Higashiyama, T.; Sakakibara, H.; Ishiguro, S. Jasmonic acid facilitates flower opening and floral organ development through the upregulated expression of SlMYB21 transcription factor in tomato. *Biosci. Biotechnol. Biochem.* **2018**, *82*, 292–303. [CrossRef] [PubMed]
56. Borges, D.F.; Lopes, E.A.; Moraes, A.R.F.; Soares, M.S.; Visôtto, L.E.; Oliveira, C.R.; Valente, V.M.M. Formulation of botanicals for the control of plant-pathogens: A review. *Crop Prot.* **2018**, *110*, 135–140. [CrossRef]
57. Podaralla, S.; Perumal, O. Influence of Formulation Factors in the Precipitation of Zein Nanoparticles. *AAPS PharmSciTech* **2012**, *13*, 919–927. [CrossRef]
58. Parris, N.; Cooke, P.H.; Hicks, K.B. Encapsulation of Essential Oils in Zein Nanospherical Particles. *J. Agric. Food Chem.* **2005**, *53*, 4788–4792. [CrossRef]
59. Poyatos-Racionero, E.; Guarí-Borràs, G.; Ruiz-Rico, M.; Morellá-Aucejo, Á.; Aznar, E.; Barat, J.M.; Martínez-Máñez, R.; Marcos, M.D.; Bernardos, A. Towards the Enhancement of Essential Oil Components' Antimicrobial Activity Using New Zein Protein-Gated Mesoporous Silica Microdevices. *Int. J. Mol. Sci.* **2021**, *22*, 3795. [CrossRef]
60. Xiao, D.; Davidson, P.M.; Zhong, Q. Spray-dried zein capsules with coencapsulated nisin and thymol as antimicrobial delivery system for enhanced antilisterial properties. *J. Agric. Food Chem.* **2011**, *59*, 7393–7404. [CrossRef] [PubMed]
61. Wu, Y.; Luo, Y.; Wang, Q. Antioxidant and antimicrobial properties of essential oils encapsulated in zein nanoparticles prepared by liquid–liquid dispersion method. *LWT* **2012**, *48*, 283–290. [CrossRef]
62. Li, K.K.; Yin, S.W.; Yang, X.Q.; Tang, C.H.; Wei, Z.H. Fabrication and characterization of novel antimicrobial films derived from thymol-loaded zein–sodium caseinate (SC) nanoparticles. *J. Agric. Food Chem.* **2012**, *60*, 11592–11600. [CrossRef]
63. Gonçalves, J.; Torres, N.; Silva, S.; Gonçalves, F.; Noro, J.; Cavaco-Paulo, A.; Ribeiro, A.; Silva, C. Zein impart hydrophobic and antimicrobial properties to cotton textiles. *React. Funct. Polym.* **2020**, *154*, 104664. [CrossRef]
64. Irache, J.M.; González-Navarro, C.J. Zein nanoparticles as vehicles for oral delivery purposes. *Nanomedicine* **2017**, *12*, 1209–1211. [CrossRef]
65. Ibáñez, M.D.; López-Gresa, M.P.; Lisón, P.; Rodrigo, I.; Bellés, J.M.; González-Mas, M.C.; Blázquez, M.A. Essential Oils as Natural Antimicrobial and Antioxidant Products in the Agrifood Indus. *Nereis* **2020**, *12*, 55–69. [CrossRef]
66. Choudhary, P.; Aggarwal, P.R.; Rana, S.; Nagarathnam, R.; Muthamilarasan, M. Molecular and metabolomic interventions for identifying potential bioactive molecules to mitigate diseases and their impacts on crop plants. *Physiol. Mol. Plant Pathol.* **2021**, *114*, 101624. [CrossRef]
67. Torres, M.A. ROS in biotic interactions. *Physiol. Plant.* **2010**, *138*, 414–429. [CrossRef]

68. Bhattarai, K.; Louws, F.J.; Williamson, J.D.; Panthee, D.R. Differential response of tomato genotypes to *Xanthomonas*-specific pathogen-associated molecular patterns and correlation with bacterial spot (*Xanthomonas perforans*) resistance. *Hortic. Res.* **2016**, *3*, 16035. [CrossRef]
69. Chandrashekar, S.; Umesha, S. Induction of antioxidant enzymes associated with bacterial spot pathogenesis in tomato. *Int. J. Food Agric. Vet. Sci.* **2012**, *2*, 22–34.
70. Silveira, P.R.; Nascimento, K.J.T.; Andrade, C.C.L.; Bispo, W.M.S.; Oliveira, J.R.; Rodrigues, F.A. Physiological changes in tomato leaves arising from *Xanthomonas gardneri* infection. *Physiol. Mol. Plant Pathol.* **2015**, *92*, 130–138. [CrossRef]
71. Zeiss, D.R.; Mhlongo, M.I.; Tugizimana, F.; Steenkamp, P.A.; Dubery, I.A. Metabolomic profiling of the host response of tomato (*Solanum lycopersicum*) following infection by *Ralstonia solanacearum*. *Int. J. Mol. Sci.* **2019**, *20*, 3945. [CrossRef]
72. García-Andrade, J.; González, B.; Gonzalez-Guzman, M.; Rodriguez, P.L.; Vera, P. The role of ABA in plant immunity is mediated through the PYR1 receptor. *Int. J. Mol. Sci.* **2020**, *21*, 5852. [CrossRef]
73. Lievens, L.; Pollier, J.; Goossens, A.; Beyaert, R.; Staal, J. Abscisic acid as pathogen effector and immune regulator. *Front. Plant Sci.* **2017**, *8*, 587. [CrossRef]
74. Sánchez-Vallet, A.; López, G.; Ramos, B.; Delgado-Cerezo, M.; Riviere, M.P.; Llorente, F.; Fernández, P.V.; Miedes, E.; Estevez, J.M.; Grant, M.; et al. Disruption of abscisic acid signaling constitutively activates *Arabidopsis* resistance to the necrotrophic fungus *Plectosphaerella cucumerina*. *Plant Physiol.* **2012**, *160*, 2109–2124. [CrossRef]
75. Ramegowda, V.; Senthil-Kumar, M.; Udayakumar, M.; Mysore, K.S. A high-throughput virus-induced gene silencing protocol identifies genes involved in multi-stress tolerance. *BMC Plant Biol.* **2013**, *13*, 193. [CrossRef] [PubMed]
76. Li, R.; Li, Y.; Zhang, Y.; Sheng, J.; Zhu, H.; Shen, L. Transcriptome analysis reveals that SlNPR1 mediates tomato fruit resistance against *Botrytis cinerea* by modulating phenylpropanoid metabolism and balancing ROS homeostasis. *Postharvest Biol. Tec.* **2021**, *172*, 111382. [CrossRef]
77. Mysore, K.S.; D'Ascenzo, M.D.; He, X.; Martin, G.B. Overexpression of the disease resistance gene Pto in tomato induces gene expression changes similar to immune responses in human and fruitfly. *Plant Physiol.* **2003**, *132*, 1901–1912. [CrossRef] [PubMed]